Measurement-Induced Localization of an Ultracold Lattice Gas

Y. S. Patil, S. Chakram, and M. Vengalattore

Phys. Rev. Lett. **115**, 140402 — Published 2 October 2015

DOI: 10.1103/PhysRevLett.115.140402

Measurement-induced localization of an ultracold lattice gas

Y. S. Patil, S. Chakram and M. Vengalattore
*Laboratory of Atomic and Solid State Physics, Cornell University, Ithaca, NY 14853**

The process of measurement can modify the state of a quantum system and its subsequent evolution. Here, we demonstrate the control of quantum tunneling in an ultracold lattice gas by the measurement backaction imposed by the act of imaging the atoms, i.e. light scattering. By varying the rate of light scattering from the atomic ensemble, we show the crossover from the weak measurement regime, where position measurements have little influence on tunneling dynamics, to the strong measurement regime, where measurement-induced localization causes a large suppression of tunneling - a manifestation of the Quantum Zeno effect. Our study realizes an experimental demonstration of the paradigmatic Heisenberg microscope and sheds light on the implications of measurement on the coherent evolution of a quantum system.

A fundamental distinction between a classical and a quantum system is its response to a measurement. While a classical system can be measured to arbitrary precision with negligible concomitant backaction, the act of measurement has profound consequences on the subsequent evolution of a quantum system [1]. In the extreme limit, a sequence of rapid, projective measurements can freeze the decay of an unstable quantum system [2–5], suppress its coherent evolution [6, 7] or confine such coherences to Hilbert subspaces demarcated by measurement-induced boundaries [8–10]. These phenomena are different manifestations of the Quantum Zeno Effect (QZE) [11, 12]. In addition to its foundational implications on the nature of quantum mechanics and the measurement process, the QZE has also garnered attention as a means of stabilizing fragile quantum states, studying emergent classicality in a quantum system due to measurement [13–15] and for controlling the thermodynamic properties of an isolated quantum system [16].

In a broader context, a measurement can be regarded as an interaction between a quantum system and a bath whose intrinsic, spatial and dynamical properties can be precisely engineered. As such, measurements can be used to coax a quantum system into novel collective phases and non-equilibrium states that might otherwise be inaccessible through more conventional means of cooling or state preparation. This is of particular relevance for ultracold atomic and molecular gases in optical lattices which have emerged as pristine realizations of correlated quantum many-body systems [17]. The inherent control and tunability of various properties of these gases have allowed for a diverse range of studies focused on the realization of ultracold analogues of correlated electronic materials [18], studies of non-equilibrium dynamics of isolated quantum many-body systems [19], and the creation of novel many-particle states of matter.

In this work, we use a two-photon *in situ* lattice imaging technique to demonstrate the measurement-induced control of quantum tunneling in an ultracold lattice gas. In contrast to molasses-based lattice imaging schemes, our imaging technique extracts fluorescence from the lattice gas while retaining the atoms in the ground vibrational band of the lattice [20]. By extending this technique down to shallow lattice depths with correspondingly large tunneling rates, we show that the process of imaging has the concomitant effect of dramatically changing the tunneling dynamics. By taking advantage of the large dynamic range of photon scattering rates that are made available by our technique, we observe the continuous crossover of tunneling dynamics from the 'weak measurement' regime, where the act of measurement exerts negligible backaction on the lattice gas, to the 'strong measurement' or Quantum Zeno regime, where the act of measurement localizes an atom to a lattice site and leads to a strong suppression of tunneling.

The principle of the imaging scheme is depicted in Fig. 1. Raman sideband cooling (RSC) [21–24] is used to cool atoms within an optical lattice to the lowest vibrational band while simultaneously pumping them to the high field seeking spin state $|D\rangle \equiv |F = 1, m_F = 1; \nu = 0\rangle$. This state is decoupled from the light field and as such, does not emit fluorescence. As shown in [20], fluorescence can be induced by shining an auxiliary 'imaging' beam that controllably promotes the atoms to a bright state $|B\rangle$ and subsequently re-cooling them back to $|D\rangle$ (see Fig. 1(a)).

The fluorescence emitted by the atoms can, in principle, be captured by a detector and thus constitutes a position measurement of the emitting atom. While such position measurements nominally impart energy to the atom as a measurement backaction, the simultaneous use of RSC mitigates this increase in energy by cycling the atoms back to the lowest vibrational band. Due to this cycling, fluorescence can be repeatedly extracted from an atom while restoring it to its original state. We introduce a position measurement rate Γ_m which we define to be the scattering rate of photons from the imaging beam, and note that this underestimates the actual scattering rate since it neglects the spontaneous emissions during the subsequent re-cooling of atoms to $|D\rangle$.

In shallow lattices, the atoms can coherently tunnel across sites at a rate J that is exponentially dependent on the lattice parameter $s = U_0/E_r$, where U_0 is the depth of the lattice and E_r is the recoil energy [25]. For

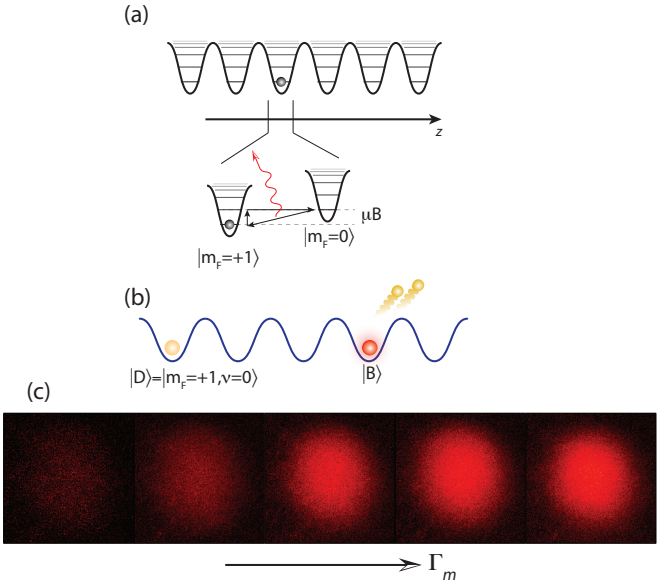

FIG. 1. (a) Lattice imaging scheme : An atom within a lattice site is cooled to the ground state $|D\rangle \equiv |F = 1, m_F = +1; \nu = 0\rangle$ via RSC. This state is nominally a 'dark state', i.e. it does not emit fluorescence. An auxiliary 'imaging' beam promotes the atom out of this state to a fluorescing state $|B\rangle$ which is subsequently cooled back to $|D\rangle$. Repeated cycles of this process extract fluorescence from the atom while continually restoring the atom to $|D\rangle$. (b) The imaging scheme thus allows us to distinguish between two possible states of the atom - a bright state $|B\rangle$ that can be imaged and a dark state $|D\rangle$ that cannot be imaged. (c) Fluorescence images of a lattice gas obtained at increasing levels of the measurement rate Γ_m. The field of view of each frame is 250 μm × 250 μm.

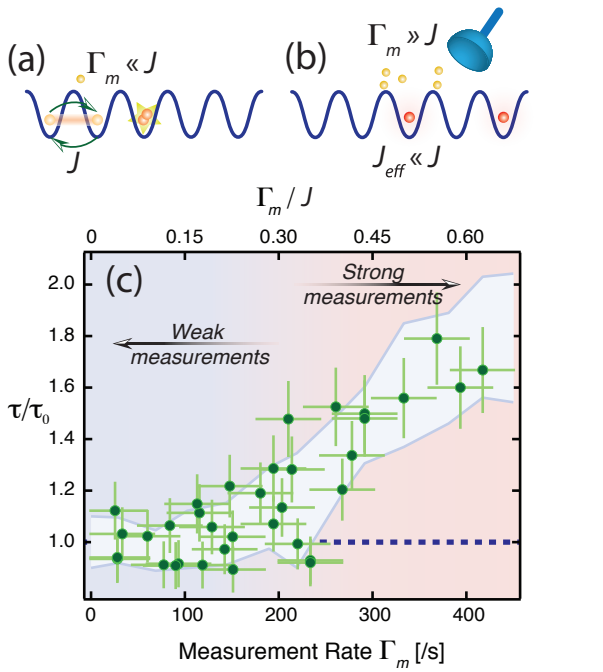

FIG. 2. Photoassociation measurements demonstrating the crossover from the weak measurement regime ($\Gamma_m \ll J$) to the strong measurement regime ($\Gamma_m \gg J$). In the former regime (a), position measurements have little influence on tunneling and the two-body lifetime $\tau = \kappa^{-1}$ is independent of the imaging rate. In the latter regime (b), measurement-induced localization suppresses tunneling rates leading to an increase of the two-body lifetime. (c) Measurements of two-body lifetime *vs* measurement rate. These data were obtained at a lattice parameter $s = 8.5(2.0)$ with $\tau_0 = 31(3)$ ms.

the filling fractions in this work ($f \sim 0.25$), such tunneling events frequently lead to multiply-occupied lattice sites at a rate $\Gamma_2 = 4qJf$ where $q = 6$ is the number of nearest neighbours in the 3D lattice [26]. In the presence of the near-resonant light used for fluorescence imaging, such multiply-occupied sites are susceptible to photoassociation and subsequent atom loss at a rate $\kappa_{PA} = \beta \int |w_0(r)|^4 d^3r \approx (0.1 - 0.3) \times \Gamma_m$ (see SI). Here, β is the photoassociation rate coefficient and $w_0(r)$ is the ground band Wannier function. Thus, the effective two-body loss rate is $\kappa = \Gamma_2 \kappa_{PA}/(\Gamma_2 + \kappa_{PA})$. For our studies described here, we typically operate in the regime $\Gamma_2 \ll \kappa_{PA} < \Gamma_m$. In other words, the formation of multiply occupied sites, at the rate Γ_2, is the rate limiting step for photoassociative loss, i.e. $\kappa \approx \Gamma_2$. Based on these rates, we identify photoassociation loss as a sensitive probe of multiply-occupied sites and hence, the tunneling rate of atoms within the lattice.

Coherent tunneling of atoms within the lattice can be strongly influenced by continuous projective measurements of atomic position. Depending on the relative magnitudes of the tunneling rate J and the measurement rate Γ_m, we can identify two distinct regimes. In the weak measurement limit $\Gamma_m \ll J$, the sporadic position measurements have negligible influence on tunneling, and the photoassociation rate κ is independent of the measurement rate (Fig. 2(a)).

In the strong measurement limit $\Gamma_m \gg J$, repeated fluorescence emission events continually project the atom into the same lattice site. In our experiments, the wavelength of the emitted photon is commensurate with the lattice spacing. As such, atoms are localized to within a lattice site subsequent to the emission of a photon. This frequent and stochastic localization [27] leads to an incoherent diffusion of atoms within the lattice at an 'effective' tunneling rate given by $\tilde{J}_{eff} \sim J^2/\Gamma_m$ [28, 29]. In other words, the effective tunneling rate $\tilde{J}_{eff}$, the rate of multiple-occupied sites Γ_2, and hence the two-body loss rate κ, monotonically decrease with increasing measurement rate. In essence, the act of observation 'freezes' the lattice gas (Fig. 2(b)). This quantum phenomenon, which does not have a classical equivalent, is a manifestation of the Quantum Zeno effect.

In our experiments, we prepare ultracold gases in the

ground vibrational band of a 3D lattice (see SI). In the absence of the imaging sequence, the lattice gas has a characteristic two-body lifetime τ_0 that is dependent on the lattice depth (and corresponding 'bare' tunneling rate) and residual light scattering due to Raman sideband cooling. In the simultaneous presence of sideband cooling, the lattice gas is subjected to either continuous or pulsed position measurements by the lattice imaging sequence at various photon scattering rates. The scattering rate is calibrated based on the measured power, beam profile and polarization of the imaging beam, and its orientation relative to the ambient magnetic field. At the lowest rates, allowing for various losses and stray light scattering, we estimate that this calibration is accurate to within a factor of two. This rate can be tuned over a large dynamic range ($\mathcal{O}(10^4)$) by varying the intensity of the imaging beam that induces fluorescence, allowing us to probe both the weak and strong measurement limits as well as the crossover regime.

At low rates of imaging, we observe that the two-body lifetime is unchanged by measurement, reflecting the negligible influence of photon scattering on coherent tunneling. However, as the imaging rates increase, the two-body lifetime of the lattice gas is seen to grow (Fig. 2(c)). This reflects the crossover from the weak measurement regime to the strong measurement regime where now, the measurement-induced localization of the atoms is the dominant influence on tunneling dynamics. This crossover regime offers a novel platform for quantitative studies of measurement-induced emergent classicality in a quantum system.

As the rate Γ_m is made much larger than the coherent tunneling rate J, we observe the expected behavior of the effective tunneling rate $J_{eff} \sim J^2/\Gamma_m$. The measured lattice lifetime grows in linear proportion to the measurement rate (Fig. 3(a)). This is a characteristic signature of the Quantum Zeno effect, i.e. increasing the rate of fluorescence *decreases* the photoassociation rate. This suppression of tunneling can also be regarded as arising from the spectral broadening of atomic eigenstates within a lattice site when the measurement-induced width of the eigenstate becomes larger than the bare tunneling rate J. Also, by confining the lattice gas at varying depths while imaging the atoms at constant measurement rate, we show the quadratic dependence of the photoassociation rate with the bare tunneling rates (Fig. 3(b)). The latter are estimated within the tight-binding model based on our calibration of the imposed lattice depth.

We note that two-body loss can also be suppressed due to an effective repulsion arising from dissipative two-body interactions such as photoassociation (also see for example, [3–5]). This can be regarded as a continuous Zeno effect and is distinct from the imaging-induced localization observed in our work. To further clarify this distinction, we measure the diffusion rate of atoms within the lattice under the influence of the imaging light. A short,

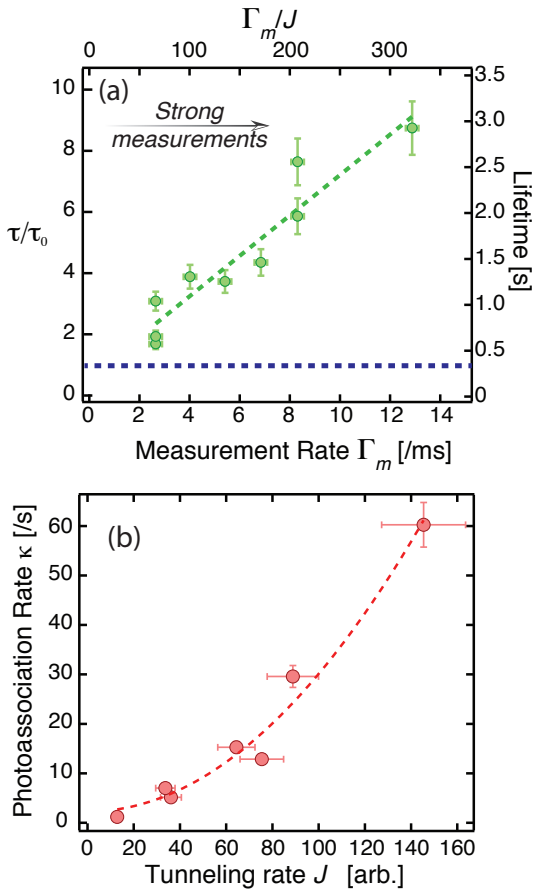

FIG. 3. In the strong measurement regime, the effective tunneling rate is given by $\tilde{J}_{eff} \sim J^2/\Gamma_m$. This leads to a two-body lifetime $\tau = \kappa^{-1}$ that linearly increases (as seen in (a)) with the measurement rate - a clear signature of the QZE. These data were obtained for $s = 23(2)$. (b) The quadratic scaling of the effective tunneling rate (and hence, the photoassociation rate κ) with the bare lattice tunneling rate is demonstrated by measurements of κ for lattice gases confined in different lattice depths. These data were obtained by imaging the lattice gases at fixed measurement rate Γ_m. The dashed line shows a quadratic fit to the data.

focused burst of on-resonant light is used to deplete the central region of the gas (Fig. 4(a,b)). Following this, the lattice depth is lowered to $s = 8.5$ to allow the atoms to repopulate the central region by tunneling. The population in this central region is quantified by absorption images of the gas at varying evolution times. In the absence of imaging, the central region is repopulated over timescales of 200-500 ms. In contrast, atomic diffusion is suppressed by imaging (Fig. 4(c)), clearly demonstrating localization of the atoms due to light scattering.

At first glance, it would appear that an atom can be localized to a lattice site for arbitrary lengths of time for sufficiently large photon scattering rates. However, in general, the act of position measurement causes the atom's energy to increase linearly with time [30]. In

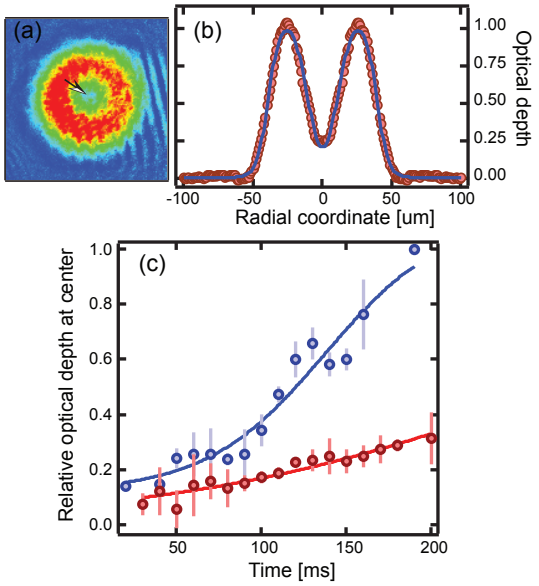

FIG. 4. Suppression of atomic diffusion due to position measurements. A brief on-resonant optical pulse depletes the central region of the lattice gas (indicated by arrow in (a)). (b) Cross section of the atomic ensemble following this pulse. (c) Atoms rapidly diffuse into this central region in the absence of imaging (blue, $s = 8.5$, $\Gamma_m = 0$). In contrast, diffusion is suppressed when the atoms are continuously imaged (red, $s = 8.5$, $\Gamma_m = 1000$ s^{-1}.)

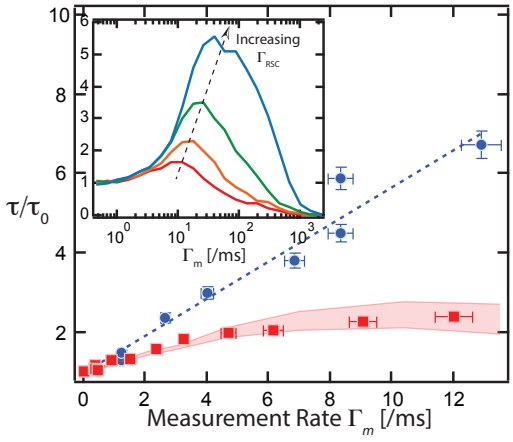

FIG. 5. For measurement rates Γ_m that exceed the Raman cooling rate Γ_{RSC}, atoms are promoted to higher vibrational bands due to the measurement. The increased tunneling rates in these higher bands cause a deviation from the linear scaling of the lifetime τ with Γ_m. Due to the proportionate relation between the Raman cooling rate and the lattice depth, this deviation occurs more readily for atoms in shallow lattices. The data shown represent two-body lifetimes in the Zeno regime for lattice parameters $s = 9.5(1.5)$, (■), $s = 21(2)$, (•). The shaded region represents a Monte Carlo simulation of a kinetic model of the measurement process. Inset: Simulated two-body lifetimes *vs* measurement rate : the onset of higher-band tunneling occurs at larger Γ_m for increasing Raman cooling rates (bottom to top).

our scheme, this increase in energy is mitigated by the simultaneous use of sideband cooling at a rate Γ_{RSC}. For measurement rates that are comparable to this cooling rate, there is a significant contribution from higher vibrational bands with correspondingly larger rates of tunneling [31]. This causes a deviation from the linear growth of two-body lifetime with measurement rate (Fig. 5). Monte Carlo simulations of a non-interacting model of this competition between measurement-induced heating and Raman cooling are in good qualitative agreement with our observations. In the regime $\Gamma_m \gg \Gamma_{RSC}$, the measurement-induced heating dominates any cooling mechanism and the atom is completely delocalized due to rapid higher-band tunneling, leading to high rates of photoassociation (Fig. 5 (inset)). Based on these considerations, it is clear that the Zeno effect is most readily seen for the regime $J \ll \Gamma_m \ll \Gamma_{RSC}$.

In summary, we use an *in situ* lattice imaging technique to demonstrate the measurement-induced localization of an ultracold lattice gas. By varying the rate of imaging, i.e. position measurements, in relation to the tunneling rate within the lattice, we show the smooth crossover from the weak measurement regime where the act of observation causes negligible backaction on the lattice gas, to the strong measurement or Zeno regime where measurement-induced localization causes a strong suppression of coherent tunneling. The large dynamic range and quantum-limited tunability inherent to this imaging scheme should enable new forms of measurement-induced control of a lattice gas by spatially and dynamically varying measurement landscapes.

In addition to shedding light on the nature of measurements and their influence on coherent quantum evolution, we also note the relevance of this study in the context of state preparation in ultracold many-body systems. While the isolation of such systems from the environment has notably allowed for the observation of various forms of long-lived mesoscopic quantum behavior, this decoupling also stymies the creation of low entropy states within experimentally viable timescales. The phenomena observed here could lead to new techniques of backaction-induced cooling, state preparation and spatially-resolved entropy segregation in a lattice gas.

This work was supported by the ARO MURI on Non-equilibrium Many-body Dynamics (63834-PH-MUR), the DARPA QuASAR program through a grant from the ARO and the Cornell Center for Materials Research with funding from the NSF MRSEC program (DMR-1120296). We acknowledge valuable discussions with H. F. H. Cheung and I. S. Madjarov. M. V. acknowledges support from the Alfred P. Sloan Foundation.

* mukundv@cornell.edu

[1] V. B. Braginsky and F. Y. Khalili, *Quantum Measurement* (Cambridge University Press, 1999).

[2] M. C. Fischer, B. Gutierrez-Medina, and M. G. Raizen, Phys. Rev. Lett. **87**, 040402 (2001).

[3] N. Syassen, D. M. Bauer, M. Lettner, T. Volz, D. Dietze, J. J. Garcia-Ripoll, J. I. Cirac, G. Rempe, and S. Dürr, Science **320**, 1329 (2008).

[4] B. Yan, S. A. Moses, B. Gadway, J. P. Covey, K. R. A. Hazzard, A. M. Rey, D. S. Jin, and J. Ye, Nature **501**, 521 (2013).

[5] G. Barontini, R. Labouvie, F. Stubenrauch, A. Vogler, V. Guarrera, and H. Ott, Phys. Rev. Lett. **110**, 035302 (2013).

[6] E. W. Streed, J. Mun, M. Boyd, G. K. Campbell, P. Medley, W. Ketterle, and D. E. Pritchard, Phys. Rev. Lett. **97**, 260402 (2006).

[7] J. M. Raimond, P. Facchi, B. Peaudecerf, S. Pascazio, C. Sayrin, I. Dotsenko, S. Gleyzes, M. Brune, and S. Haroche, Phys. Rev. A **86**, 032120 (2012).

[8] P. Facchi and S. Pascazio, Phys. Rev. Lett. **89**, 080401 (2002).

[9] F. Schäfer, I. Herrera, S. Cherukattil, C. Lovecchio, F. S. Cataliotti, F. Caruso, and A. Smerzi, Nat. Comm. **5** (2014).

[10] A. Signoles, A. Facon, D. Grosso, I. Dotsenko, S. Haroche, J. M. Raimond, M. Brune, and S. Gleyzes, Nat. Phys. **10.1038/nphys3076** (2014).

[11] B. Misra and E. C. G. Sudarshan, J. Math. Phys. **18**, 756 (1977).

[12] W. M. Itano, D. J. Heinzen, J. J. Bollinger, and D. J. Wineland, Phys. Rev. A **41**, 2295 (1990).

[13] T. Bhattacharya, S. Habib, and K. Jacobs, Phys. Rev. Lett. **85**, 4852 (2000).

[14] K. Jacobs and D. Steck, New J. Phys. **13**, 013016 (2011).

[15] J. Javanainen and J. Ruostekoski, New J. Phys. **15**, 013005 (2013).

[16] N. Erez, G. Gordon, M. Nest, and G. Kurizki, Nature **452**, 724 (2008).

[17] I. Bloch, J. Dalibard, and W. Zwerger, Rev. Mod. Phys. **80**, 885 (2008).

[18] M. Lewenstein, A. Sanpera, V. Ahufinger, B. Damski, A. Sen, and U. Sen, Adv. Phys. **56**, 243 (2007).

[19] A. Polkovnikov, K. Sengupta, A. Silva, and M. Vengalattore, Rev. Mod. Phys. **83**, 863 (2011).

[20] Y. S. Patil, S. Chakram, L. M. Aycock, and M. Vengalattore, Phys. Rev. A **90**, 033422 (2014).

[21] V. Vuletić, C. Chin, A. J. Kerman, and S. Chu, Phys. Rev. Lett. **81**, 5768 (1998).

[22] S. E. Hamann, D. L. Haycock, G. Klose, P. H. Pax, I. H. Deutsch, and P. S. Jessen, Phys. Rev. Lett. **80**, 4149 (1998).

[23] D. J. Han, S. Wolf, S. Oliver, C. McCormick, M. T. DePue, and D. S. Weiss, Phys. Rev. Lett. **85**, 724 (2000).

[24] A. J. Kerman, V. Vuletić, C. Chin, and S. Chu, Phys. Rev. Lett. **84**, 439 (2000).

[25] D. Jaksch, C. Bruder, J. I. Cirac, C. W. Gardiner, and P. Zoller, Phys. Rev. Lett. **81**, 3108 (1998).

[26] J. J. Garcia-Ripoll, S. Dürr, N. Syassen, D. M. Bauer, M. Lettner, G. Rempe, and J. I. Cirac, New J. Phys. **11**, 013053 (2009).

[27] M. Holland, S. Marksteiner, P. Marte, and P. Zoller, Phys. Rev. Lett. **76**, 3683 (1996).

[28] M. J. Gagen, H. M. Wiseman, and G. J. Milburn, Phys. Rev. A **48**, 132 (1993).

[29] J. I. Cirac, A. Schenzle, and P. Zoller, EuroPhys. Lett. **27**, 123 (1994).

[30] Y. Yanay and E. J. Mueller, Phys. Rev. A **90**, 023611 (2014).

[31] B. Zhu, B. Gadway, M. Foss-Feig, J. Schachenmayer, M. L. Wall, K. R. A. Hazzard, B. Yan, S. A. Moses, J. P. Covey, D. S. Jin, J. Ye, M. Holland, and A. M. Rey, Phys. Rev. Lett. **112**, 070404 (2014).